Journal of Environmental Management 413 (2026) 130427

Contents lists available at ScienceDirect

Journal of Environmental Management

journal homepage: www.elsevier.com/locate/jenvman

Research article

Linking nitrogen transformations and soil $\delta^{15}N$ to assess drivers of nitrogen losses across a tropical peat swamp forest and an oil palm plantation

Elizabeth Gachibu Wangari [a,*], Kien Yung Teo [b,c], Ricky Mwangada Mwanake [a], Faustina Elfrida Sangok [c], Herman Umbau Lindang [c], Auldry Chaddy [c], Sharon Yu Ling Lau [c], Fawad Khan [a], Nur Azima Busman [c], Kim San Lo [c], Hanna Vahter [b], Muhammad Kamil-Sardar [b], Kärt Kanger [b], Georg Willibald [a], Per Ambus [d,e], Mari Pihlatie [f], Kaido Soosaar [b], Mikk Espenberg [b], Klaus Butterbach-Bahl [a,e], Ralf Kiese [a], Ülo Mander [b], Lulie Melling [c]

[a] Karlsruhe Institute of Technology (KIT), Institute for Meteorology and Climate Research, Atmospheric Environmental Research (IMK-IFU), Kreuzeckbahnstrasse 19, Garmisch-Partenkirchen, 82467, Germany
[b] Department of Geography, Institute of Ecology and Earth Sciences, University of Tartu, Vanemuise St. 46, Tartu, 51003, Estonia
[c] Sarawak Tropical Peat Research Institute, Lot 6035, Kuching-Samarahan Expressway, Kota Samarahan, Sarawak, 94300, Malaysia
[d] Department of Geosciences and Natural Resource Management, University of Copenhagen, Copenhagen, 1350, Denmark
[e] Center for Landscape Research in Sustainable Agricultural Futures (Land-CRAFT), Department of Agroecology, Aarhus University, Denmark
[f] Department of Agricultural Sciences, Institute of Atmospheric and Earth System Research, University of Helsinki, PO Box 56, Helsinki, 00014, Finland

ARTICLE INFO

Keywords:
Denitrification
Gross nitrification
Nitrogen leaching
Nitrogen balance
Gross ammonification
Microbial gene abundance
Nitrous oxide

ABSTRACT

Conversion of tropical peatland forests to oil palm plantations has been associated with elevated nitrous oxide (N_2O) emissions and nitrate (NO_3^-) leaching, yet the biogeochemical mechanisms driving these nitrogen (N) losses remain poorly understood. To address this gap, soil N_2O fluxes, gross N transformation rates, microbial gene abundances, annual NO_3^- leaching rates, and bulk soil $\delta^{15}N$ signatures were quantified along transects in Malaysia that included intact tropical peat swamp forest and drained oil palm plantation. Oil palm plantation sites had higher topsoil oxygen (O_2) concentrations than forest sites, indicating that drainage shifts soils from predominantly anaerobic to aerobic conditions. These redox shifts, together with fertilizer inputs, increased nitrifier gene abundances and enhanced gross nitrification rates, which exceeded ammonification rates by up to 186%, promoting soil NO_3^- accumulation. The elevated soil NO_3^- concentrations stimulated N_2O production, probably through coupled nitrification-denitrification, and increased NO_3^- leaching. Overall, these results showed that oil palm plantation sites had higher gaseous and hydrological N losses than peat forest sites. Additionally, nitrification rates, hydrological N export, and gaseous N losses were positively correlated with more enriched bulk soil $\delta^{15}N$ values along the land use gradient. These findings demonstrated that bulk soil $\delta^{15}N$ patterns may have the potential to serve as indicators of long-term N cycling and losses in tropical peatlands associated with human-induced land use changes.

1. Introduction

Tropical peatlands are globally significant reservoirs of carbon (C) and nitrogen (N), storing approximately 81.7–91.9 Gt C and 5.9–25.9 Gt N within their organic-rich soils (Page et al., 2011; Yin et al., 2022). However, expansion of oil palm cultivation, which is a major cash crop across Southeast Asia, has led to widespread conversion of peat swamp forests into intensively managed oil palm plantations, resulting in substantial losses of peat C and N stocks (Koh et al., 2011; Tonks et al., 2017; McCalmont et al., 2021). This conversion involves forest clearing, drainage, and N fertilizer use, which alter soil conditions, thereby affecting soil C and N cycling and greenhouse gas (GHG) emission (e.g., Cooper et al., 2020; Reiss et al., 2025). For example, intact tropical peat swamp forests exhibit near-zero and sometimes

* Corresponding author.
E-mail address: elizabeth.wangari@kit.edu (E.G. Wangari).

https://doi.org/10.1016/j.jenvman.2026.130427
Received 9 April 2026; Received in revised form 23 June 2026; Accepted 3 July 2026
Available online 6 July 2026

negative N_2O fluxes, whereas drained and fertilized plantations can become substantial sources of N_2O (Cooper et al., 2020; Mander et al., 2024). Mechanistically, drainage partially aerates naturally anoxic peat, stimulating nitrification and promoting incomplete denitrification, the primary sources of N_2O (Butterbach-Bahl et al., 2013). Moreover, N fertilizer application in oil palm plantations, which can exceed 100 kg N ha^{-1} yr^{-1} (Comeau et al., 2016), increases mineral N availability, and can intensify hydrological N losses relative to intact peat forests (Formaglio et al., 2020).

Despite the recognition that oil palm plantations are global hotspots of N_2O emissions, major uncertainties remain on the underlying drivers. Most previous studies in tropical peatland-oil palm plantation systems have focused on surface N_2O flux measurements (e.g., Melling et al., 2007; Cooper et al., 2020; Chen et al., 2024). While essential, such flux measurements alone provide limited mechanistic insights into how land-use conversion alters internal N turnover processes and associated pathways of N retention and loss (Pardon et al., 2016a). The quantification of gross N transformation rates, which represent the actual rates of N turnover within soils (Murphy et al., 2003), is therefore critical for evaluating whether elevated N_2O emissions and nitrate (NO_3^-) leaching arise from increased substrate supply, enhanced process rates, reduced microbial consumption, or shifts in redox constraints. However, such gross N turnover measurements have mainly been done in temperate and some tropical forest ecosystems (Verchot et al., 2001; Gütlein et al., 2016; Braun et al., 2018; Figueiredo et al., 2019), with comparatively limited application in tropical peatlands (Allen et al., 2015; Byun et al., 2024). Moreover, although O_2 availability is widely recognized as a primary control on both soil N_2O production and consumption rates, few studies have explicitly quantified how such rates may be influenced by changes in O_2 concentrations as a result of land use-induced changes in water table depth on soil aeration (Lam et al., 2022; Hatano, 2025; Midot et al., 2025).

Natural abundance soil $\delta^{15}N$ can be a strong integrative measure for tracking human-induced changes in ecosystem N turnover rates since it is well-known to serve as an indicator of N sources, transformations, and losses across various land uses (Robinson, 2001; Craine et al., 2015a, 2015b; Choi et al., 2020). Specifically, $\delta^{15}N$ signatures of soil pools reflect the cumulative effects of isotopic fractionation that occur during N cycling and loss processes (Denk et al., 2017). During these N transformations, microbes preferentially use ^{14}N, and soil N losses are also relatively ^{15}N-depleted, leaving the remaining soil N pool ^{15}N-enriched. Thus, more enriched soil $\delta^{15}N$ values are often interpreted as signals of more "open" N cycles with high N inputs and losses (e.g., Pardo and Nadelhoffer, 2010; Gurmesa et al., 2022; Wangari et al., 2024). In contrast, depleted $\delta^{15}N$ values suggest closed conservative cycles dominated by tight recycling of N between plants and soil microbes (Emmett et al., 1998; Dijkstra et al., 2006; Bai et al., 2012). Land use change, such as converting forests to agriculture, can alter soil $\delta^{15}N$ patterns by altering N inputs, transformation rates, and loss pathways (e.g., Wangari et al., 2024; Choi et al., 2020).

Although soil $\delta^{15}N$ patterns vary across tropical land use gradients (Sheng et al., 2014; Baumgartner et al., 2021), the mechanistic links between $\delta^{15}N$ signals and specific N transformation and loss processes remain poorly characterized in tropical peatlands, particularly after conversion to oil palm plantations. Such integrative approaches may be crucial for identifying the drivers of spatial heterogeneity in N cycling rates within tropical peatlands and for assessing the potential use of bulk soil $\delta^{15}N$ natural abundance as an indicator of long-term human-induced changes in ecosystem N cycling and loss pathways. To address these gaps, a detailed spatial analysis of gross N transformation and loss pathways was done across two tropical peatland land uses in Malaysia, spanning intact peat swamp forests (with contrasting phasic communities) and a drained oil palm plantation. The main objectives were: (i) to quantify land use effects on soil $\delta^{15}N$, soil N_2O fluxes, and key soil physicochemical properties, (ii) to evaluate how land use alters gross N cycling and loss processes, including ammonification, nitrification, denitrification, and N leaching, (iii) to assess the role of O_2 availability in regulating soil N_2O emissions across different land uses, and (iv) to identify the biogeochemical mechanisms driving land use effects on N cycling and N loss pathways.

2. Materials and methods

2.1. Study area

The study was conducted in a mixed landscape with tropical peatland forests and an oil palm (*Elaeis guineensis*) plantation in the Betong Division, Sarawak, Malaysia (Fig. 1). The region has a humid tropical climate, with a mean annual temperature of about 26.9 °C and a mean annual precipitation of around 2798 mm (Ishikura et al., 2018; Monda et al., 2018; Tang et al., 2019). Forest sites were located within Maludam National Park, Sarawak's largest protected peat swamp forest, covering approximately 536 km^2 (Tang et al., 2020). The forest is dominated by *Litsea* spp. and *Shorea albida* trees, with a canopy height of up to 25 m in 2010 (Wong et al., 2025). The forest floor is characterized by hummocks, hollows, microtopography, and leaf litter. Mean water table depths measured between 2011 and 2014 ranged from +15.8 to −22.2 cm relative to the peat surface (Kiew et al., 2018). Maludam peat swamp forest comprises distinct phasic communities (Anderson, 1963). Transects were established in four of these communities, namely Mixed peat swamp, Alan Batu, Alan Bunga, and Pandang Alan forests, occurring sequentially from Lupar River toward the center of the peat dome at approximately 1.2 km, 4.5 km, 5.9 km, and 8.6 km from the riverbank, respectively (Fig. 1C). Mixed peat swamp forests were at lower elevation with less woody, highly decomposed peat and higher tree diversity. Alan Batu and Alan Bunga are dominated by *Shorea albida* and contain comparatively woody peat, whereas Padang Alan occurs on less fertile, more fibrous peat with smaller-stature trees (Melling, 2016). The peat is predominantly ombrotrophic and nutrient-poor (Melling et al., 2007).

As for the oil palm plantation, conversion from secondary peat swamp forest occurred between March 2017 and April 2018, with early drainage to lower the water table for road construction and vegetation clearance (Wong et al., 2025). Peat was then compacted with a tracked excavator to increase soil bulk density, reduce palm leaning and toppling, and enhance its water-holding capacity (Melling et al., 2007). Water tables are managed at −50 to −70 cm. Oil palm seedlings were planted in May 2018 in a triangular pattern with an 8.5 m spacing between seedlings. At the time of sampling (October 2024), the oil palms were approximately 6-7 years old. Mineral fertilizer, comprising urea, ammonium sulphate, rock phosphate, muriate of potash, and micronutrients (copper, zinc, and boron), was applied to the oil palm plantation within a 2 m radius of each oil palm trunk. The nitrogen fertilizers were applied at an annual rate of approximately 116 kg N ha^{-1} yr^{-1} in two equal split applications (e.g., Tarmizi and Mohd Tayeb, 2006; Melling et al., 2013; Skiba et al., 2020). Peat depth at the plantation ranged from approximately 530 to 650 cm (Ratai et al., 2024).

2.2. Field campaigns and sampling design

Two campaigns were conducted in October 2024 (Campaign I) and July 2025 (Campaign II). Both occurred under relatively stable conditions (air temperatures above 26 °C and minimal rainfall during sampling). Campaign I focused on plant and soil $\delta^{15}N$, N_2O fluxes, soil physicochemical properties, and DIN leaching rates. Campaign II focused on the quantification of in-vitro N transformation rates (denitrification, gross nitrification, gross ammonification) and microbial functional gene abundances. Sampling followed structured transects to capture spatial heterogeneity (Fig. S1). Specifically, four transects were established within the Mixed peat swamp, Alan Batu, Alan Bunga, and Padang Alan forests, each with three sampling points spaced 20 m apart. In the oil palm plantation, three transects were established, each with four sampling points spaced 400 m apart (Fig. S1) to capture

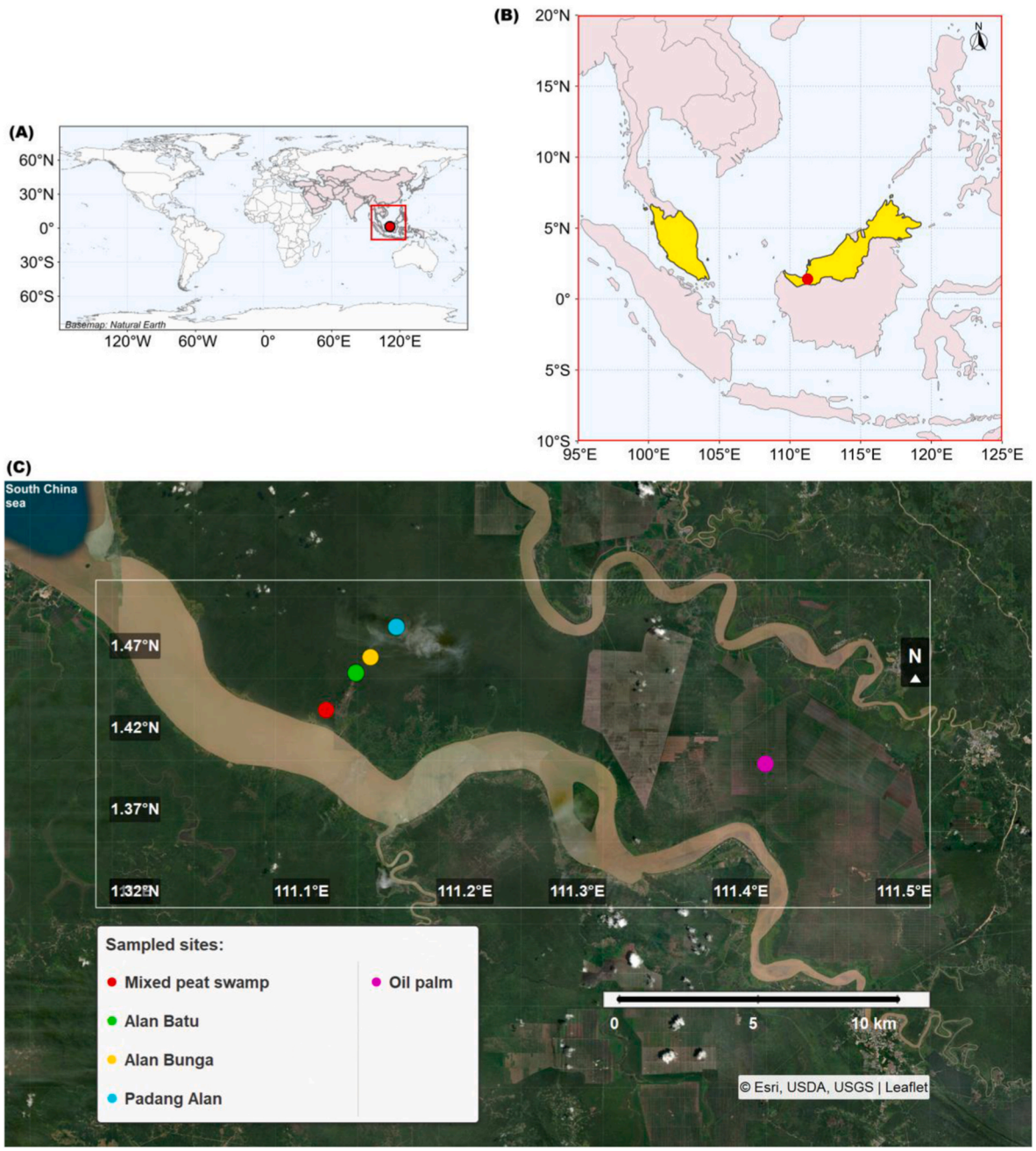

Fig. 1. Map showing the location of the study region in Malaysia within (A) Asia and (B) Southeast Asia, and (C) the location of peat swamp forest sites (Mixed peat swamp, Alan Batu, Alan Bunga, and Padang Alan) in Maludam National Park and the oil palm plantation site in Betong Division.

management heterogeneity. At each sampling point, measurements and samples were collected in triplicate.

2.3. Field measurements and laboratory analyses

2.3.1. Soil N_2O fluxes and physicochemical properties

Soil N_2O fluxes were measured in Campaign I using a closed dynamic chamber (white PVC, 65 L, Ø = 50 cm, h = 40 cm) connected to an LI-7820 N_2O/H_2O Trace Gas Analyzer (LI-COR Biosciences, Lincoln, NE, USA). Fluxes (μg N m^{-2} h^{-1}) were calculated from the linear change in headspace mixing ratios over time (Wangari et al., 2022). Soil temperature and volumetric water content were measured using a TEROS 12 sensor (METER Group, USA). Soil O_2 concentrations were measured in situ using an Oxygen Dipping Probe DP-PSt3 connected to a Fibox 4 Oxygen Meter via a polymer optical fiber (POF) (PreSens, Germany). Temperature correction for O_2 readings was performed using data from a PreSens Pt100 Temperature Probe. Soil bulk density and gravimetric moisture were determined using intact stainless-steel cores (100 cm^3) that were oven-dried at 105 °C for 24 h. For chemical analysis, soil samples were air-dried, sieved (≤2 mm), and stored at 4 °C. Soil pH was measured in a 1:2.5 (soil: water) suspension. NH_4^+ and NO_3^- ions were extracted from 5 g of soil samples with ultrapure water (25 °C and shaking at 300 rpm for an hour) and quantified by ion chromatography (Metrohm 716 Compact IC, Switzerland).

2.3.2. Plant and soil $\delta^{15}N$ and elemental composition

Foliar and peat soil samples were collected during Campaign I, oven-dried at 60 °C, ball-milled, and analyzed for organic C and total N content, and $\delta^{15}N$ using an elemental analyzer coupled to an isotope ratio mass spectrometer (EA 110, CE instruments; DELTA^{PLUS} IRMS,

Finnigan MAT). The natural abundance $\delta^{15}N$ values were reported relative to atmospheric N_2 (Equation (1)), where R_{sample} is the N ($^{15}N/^{14}N$) isotope ratio measured in the samples, and $R_{standard}$ is the isotope ratio in the standard (atmospheric N_2).

$$\delta^{15}N_{sample}\ (‰) = \left(\frac{R_{sample}}{R_{standard}} - 1\right) \times 1000 \quad (1)$$

2.3.3. Annual DIN leaching

Annual DIN leaching (NO_3-N and NH_4-N) was estimated using Amberlite ion-exchange resins (exchange capacity of ≥0.6 mmol mL^{-1}) (e.g., Sousa et al., 2016; Wangari et al., 2024). Six grams of resins were placed in each PVC tube (2 cm height, 5 cm internal diameter), covered with a permeable mesh, and installed at a depth of 30 cm in October 2024, then retrieved in October 2025. Resins were extracted with 1 M KCl (1:5), and DIN was quantified colorimetrically (Bolleter et al., 1961; Hood-Nowotny et al., 2010; Wangari et al., 2022). Annual leaching rates were then calculated based on the extracted DIN mass and the surface area of each resin tube, as in Equation (2) from Wangari et al. (2024).

$$DIN\ leaching\ rate\ \left(kg\ ha^{-1}\ yr^{-1}\right) = \frac{Extract\ concentration\ \left(mg\ L^{-1}\ yr^{-1}\right) \times Volume\ of\ extract\ (L) \times 10^{-6}}{Resin\ tube\ surface\ area\ (ha)} \quad (2)$$

2.3.4. Denitrification and gross N transformation rates

Denitrification rates (N_2 and N_2O) and N_2O: (N_2O + N_2) product ratios were quantified (Campaign II) using intact soil cores (100 cm^3; 5 cm depth) in a helium incubation system at 26 °C (Butterbach-Bahl et al., 2002). Incubations were conducted sequentially at 20%, 15%, 10%, 5%, and 0% oxygen levels to cover the range of field-observed O_2 conditions. Fluxes were calculated from linear concentration changes and expressed as μg N g^{-1} d^{-1}.

Gross ammonification rates (GAR) and gross nitrification rates (GNR) were measured (Campaign II) using ^{15}N pool dilution (Murphy et al., 2003; Ramm et al., 2022; Khan et al., 2025). Homogenized soils (roots removed) were amended with ^{15}N-labeled $(NH_4)_2SO_4$ (for GAR) or $K^{15}NO_3$ (for GNR). Subsamples were extracted immediately (T0) and after 24 h of incubation at 26 °C (T1) with 1 M KCl. Total DIN concentrations were measured colorimetrically, and ^{15}N-NH_4/^{15}N-NO_3 concentrations were determined using REOX/MIMS on a membrane inlet mass spectrometer (Kana et al., 1994; Lin et al., 2017; Mwanake et al., 2026). Gross nitrification and ammonification rates in μg N g^{-1} d^{-1} were then calculated using equations in Murphy et al. (2003).

2.3.5. DNA extraction and qPCR

DNA was extracted from Campaign II composite soil using the DNeasy PowerSoil Pro kit (Qiagen, Germany) with bead beating (Precellys® 24; 5000 rpm for 20 s). The quality and concentration of the extracted DNA were assessed spectrophotometrically, and the DNA extracts were stored at −20 °C. Quantitative qPCR(Rotor-Gene® Q, Qiagen) quantified bacterial and archaeal 16S rRNA genes and key functional genes for nitrification (*amoA*, including comammox), denitrification (prokaryotic *nirS*, *nirK*, *nosZ-I*, and *nosZ-II*, and fungal *nirK*), dissimilatory nitrate reduction to ammonium (DNRA) (*nrfA*), and N-fixation (*nifH*) processes. Amplifications were performed in 10 μL reaction mixtures containing 5 μL of Maxima SYBR Green Master Mix (Thermo Fisher Scientific Inc., USA), optimized concentrations of forward and reverse primers, 1 μL of template DNA, and sterile distilled water. The gene-specific primer sets, optimized primer concentrations, and thermal cycling conditions for each target gene are listed in Espenberg et al. (2024). Standard curves for each target gene were generated from serially diluted stock solutions of the target sequences (Eurofins MWG Operon, Germany). Quantitative data were analyzed using RotorGene Series Software (version 2.0.2, Qiagen, Hilden, Germany) and the LinRegPCR program v. 2021.2 (Ruijter et al., 2009). Gene abundances were calculated as the mean fold differences between the samples and the corresponding 10-fold standard dilution in the respective standard curves, following Ruijter et al. (2009). Gene abundances are expressed as gene copy numbers per gram of soil dry weight (gene copies g^{-1} dw).

2.4. Statistical analysis

Significant land use and depth-related differences in soil properties, $\delta^{15}N$ isotopic patterns, N_2O fluxes, and in-vitro N turnover rates were determined using the non-parametric Dunn's post hoc test ($P < 0.05$). To determine the mechanistic drivers of spatial variability in the data, a principal component analysis (PCA) of the key biogeochemical variables measured across the land use was conducted. The PCA utilized in-vitro GAR, GNR, denitrification rates, leaching rates, gene abundance, field-measured N_2O fluxes, and soil $\delta^{15}N$ as input variables. Before analysis, all variables were standardized (centered and scaled to have a mean of 0 and standard deviation of 1) to ensure comparability across variables with different units and scales. The PCA ordination was generated using the correlation matrix, enabling direct visualization of how various components of biogeochemical N cycling and loss pathways co-vary across land use gradients. Bivariate relationships among these variables were further assessed using simple linear regression analyses to provide a more nuanced assessment of biogeochemical linkages. All these analyses were performed in R statistical software version 4.5.1 (R Core Team, 2025).

3. Results

3.1. Influence of land use on physico-chemical parameters, N_2O fluxes, and annual N leaching

Topsoil (0–10 cm) and foliar properties differed markedly between the oil palm plantation and peat swamp forest sites (Fig. 2; Table S1). Overall, variability in soil physico-chemical properties was greater among the forest sites than among the plantation sites. Soils were strongly acidic across all sites (pH 3.0 to 4.2), with a tendency toward higher mean pH in forest soils, although differences were not statistically significant (Table S1). SWC was up to 2.6 times higher in forests than in the plantation sites, whereas soil O_2 concentrations were approximately two orders of magnitude higher in the plantation than in forest soils. Consistent with these differences, soil NH_4-N concentrations were up to an order of magnitude higher in the forest than in the plantation sites. Within the forest sites, NH_4-N was higher at the Mixed peat swamp and Alan Batu than at Padang Alan sites. In contrast, soil NO_3-N concentrations were up to two orders of magnitude higher in the plantation than in forest soils, and NO_3-N: NH_4-N ratios were similarly elevated in plantation soils.

Forested sites had higher soil organic carbon, soil nitrogen, and soil C: N ratios than plantation soils, while bulk soil $\delta^{15}N$ values were significantly more enriched in plantation soils (Table S1; Fig. 2G and H). This trend was also consistent across all bulk $\delta^{15}N$ analyses of green leaves, leaf litter, and soil layers, which were higher at the plantation sites than at the forest sites (Fig. S2). Among the forest sites, the Mixed

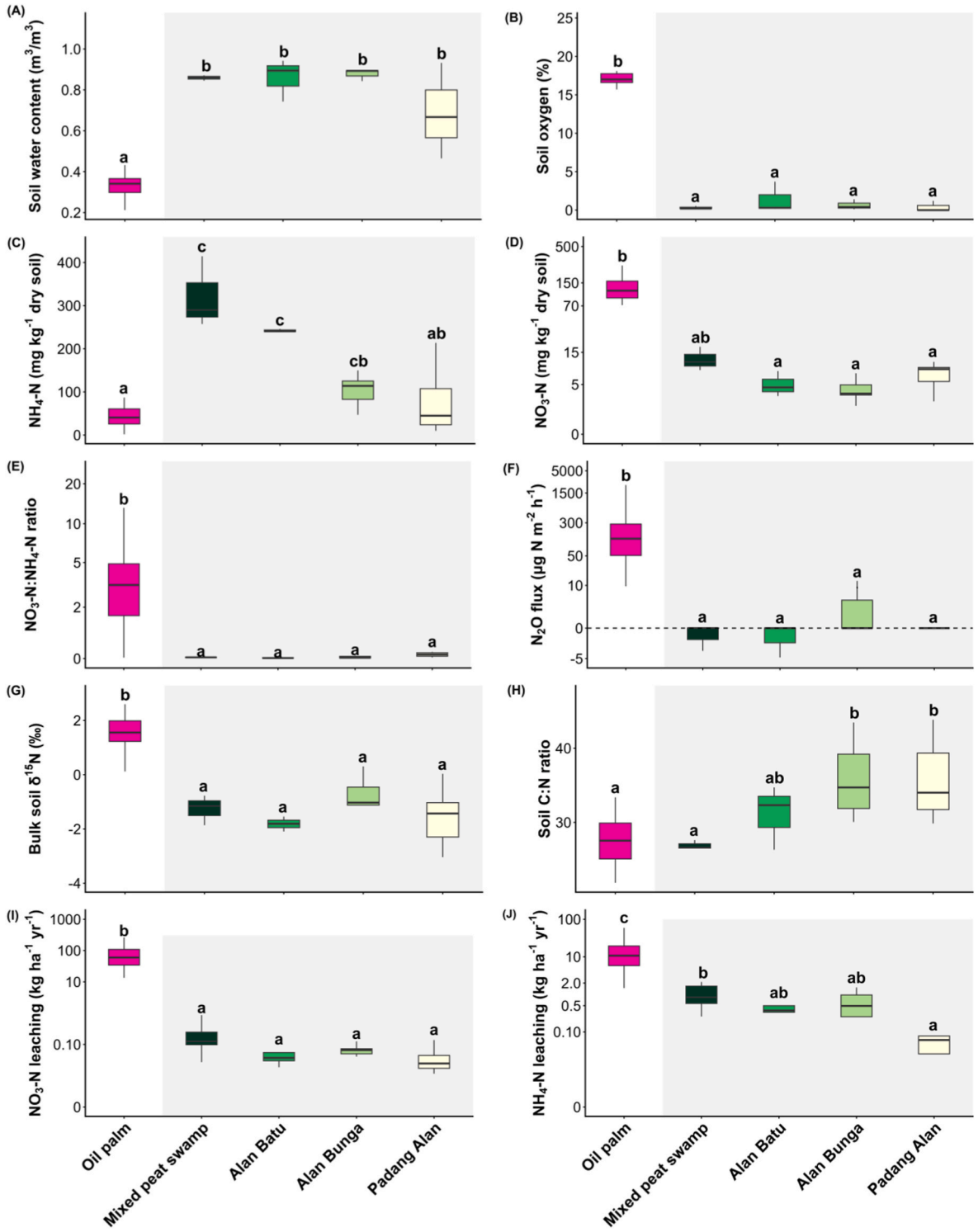

Fig. 2. Variation in topsoil (0–10 cm) physicochemical properties, field N_2O fluxes (Campaign I), and annual dissolved inorganic nitrogen (DIN) leaching across the oil palm plantation and forest sites. Different lowercase letters above the boxplots indicate significant differences among sites (Kruskal–Wallis test followed by Dunn's post hoc test; $P < 0.05$).

peat swamp forest profile exhibited higher bulk $\delta^{15}N$ values, particularly in the foliage. Overall, green leaves and leaf litter had lower bulk $\delta^{15}N$ values than the soil, and the $\delta^{15}N$ values increased with soil depth across all land uses. In contrast to bulk $\delta^{15}N$ patterns, C: N ratios were highest in the foliage of Padang Alan and Alan Bunga forest sites (Fig. S2). C: N ratios increased with soil depth in the oil palm sites but decreased with soil depth in the forested sites.

Soil N_2O fluxes ranged from −9.74 to 2405 µg N m^{-2} h^{-1}. The plantation soil was a net source of N_2O (mean = 252.9 µg N m^{-2} h^{-1}), whereas forest sites generally functioned as weak N_2O sinks (Fig. 2F; Table S1). Annual DIN leaching rates ranged from 0.01 to 59.2 kg N ha^{-1} yr^{-1} for NH_4-N and from 0.01 to 263.1 kg N ha^{-1} yr^{-1} for NO_3-N. Oil palm plantation sites exhibited up to two orders of magnitude higher NH_4-N and NO_3-N leaching than forest sites, with maximum annual DIN

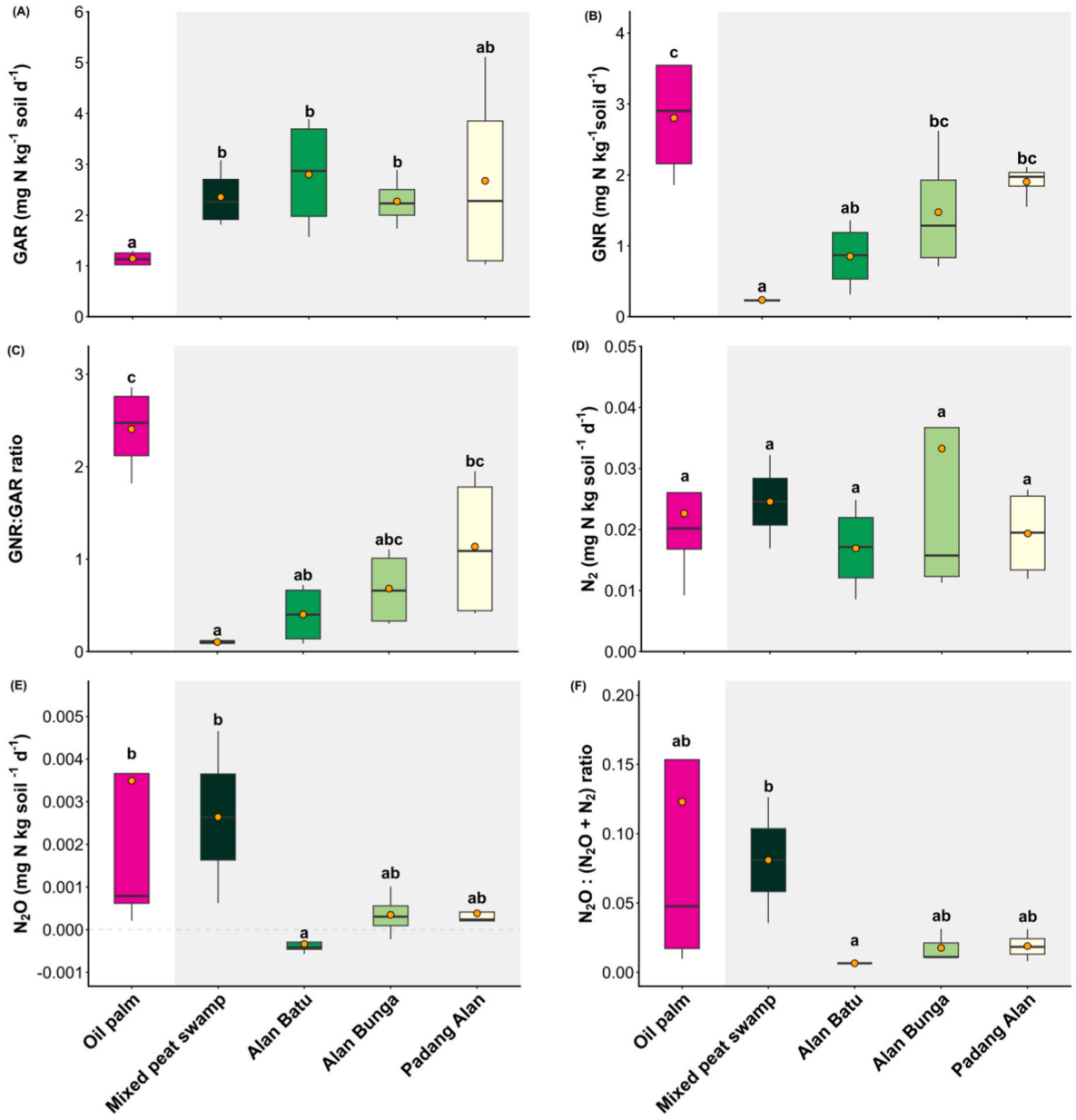

Fig. 3. Variation in (A) GAR, (B) GNR, (C) GNR:GAR ratio, and (D) denitrification rates across oil palm plantation and forest sites from in-vitro soil incubations. Lowercase letters above the boxplots indicate significant differences ($P < 0.05$) among sites based on Kruskal-Wallis test followed by Dunn's post hoc test.

leaching rates remaining below 2.6 kg N ha^{-1} yr^{-1} (Fig. 2I and J; Table S1). NO_3-N dominated DIN leaching at the plantation, accounting for 83% of mean annual DIN leaching losses (89 kg N ha^{-1} yr^{-1}) (Table S1).

3.2. Influence of land use on N transformation rates

GAR and GNR ranged from 1.03 to 3.89 mg N kg^{-1} d^{-1} and from 0.22 to 3.55 mg N kg^{-1} d^{-1}, respectively (Fig. 3; Table S2). GAR was up to 3.8 times higher in forests than in plantation sites and exhibited greater spatial variability within forests, particularly at Padang Alan. In contrast, GNR were up to 14.8 times higher in the plantation than in the forests. GNR:GAR ratios were consistently higher in plantation soils (1.82–2.86), indicating that nitrification exceeded ammonification by 82–186%. In most forest sites, ratios were less than 1. Total denitrification ($N_2O + N_2$) was substantially lower than GAR and GNR (0.01–0.11 mg N kg^{-1} d^{-1}; Table S2) and showed limited spatial variation. Denitrification products were dominated by N_2, with N_2O contributing 1–39%, as indicated by N_2O: ($N_2O + N_2$) ratios (Fig. 3; Table S2). N_2 fluxes did not differ significantly among land uses (Fig. 3D), whereas N_2O fluxes were higher in the plantation and Mixed peat swamp than in Alan Batu, consistent with differences in product ratios (Fig. 3F).

3.3. Effects of oxygen availability on denitrification rates across land uses

Besides quantifying in-vitro denitrification rates under ambient O_2 levels (Fig. 3), their changes were also examined under varying soil O_2 conditions (Fig. 4). Overall, gaseous N losses changed more substantially with decreasing soil O_2 concentrations at the plantation sites than at the forested sites. For example, while a reduction in soil O_2 from 20% to 10% showed no noticeable change in N_2 fluxes across all sites, N_2O fluxes and their product ratio increased at the plantation sites, but not at forest sites (Fig. 4A). Further reduction of soil O_2 from 10% to 0% led to an exponential increase in N_2 and N_2O fluxes at the plantation sites. The N_2O product ratio also increased substantially as soil O_2 declined from

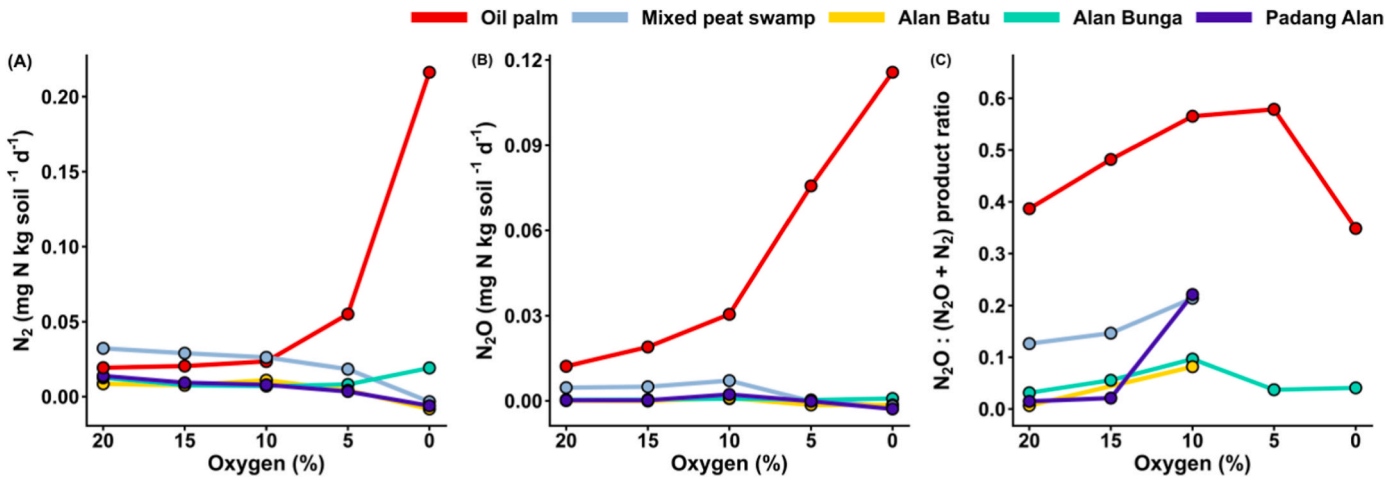

Fig. 4. Effects of O_2 availability on (A) N_2 fluxes, (B) N_2O fluxes, and (C) their product ratios across oil palm plantation and forest sites. Product ratios are not shown for Alan Bunga and Padang Alan, where either N_2O or N_2 or both had negative fluxes.

20% to 10%, showing a marginal change from 10% to 5% O_2, followed by a steep decrease when O_2 levels were decreased to zero (Fig. 4B). Unlike at the plantation sites, N_2O fluxes became negative or approached zero at the forest sites when soil O_2 concentrations were decreased to zero (Fig. 4A and B). It is noteworthy that based on in situ-measured topsoil O_2 concentrations of 17% at oil palm plantations and nearly 0% at all four forested sites (Fig. 2), the in-vitro N_2O flux directions aligned with those measured in the field, that is, soils acted as net atmospheric N_2O sources at plantation sites, while at forest sites negative or near-zero fluxes were observed in the field as well as in the laboratory measurements under observed field level O_2 concentrations (Fig. 2; Fig. 4; Fig. S2).

3.4. *Influence of land use on microbial functional gene abundance*

Functional gene abundances varied by land use (Fig. 5; Fig. S4). Ammonia-oxidation genes (*amoA*) tended to be more abundant in plantation soils and Mixed peat swamp than in Alan Batu, although these differences were not significant. In contrast, nitrite-reduction genes (*nirS*, *nirK*, fungal *nirK*) and the broader denitrification gene pool (*nirS*, *nirK*, fungal *nirK*, *nosZ-I*, *nosZ-II*) were generally more abundant in forest soils than in plantation soils. Similarly, *nifH* abundances were higher in the forest than in plantation soils (Fig. 5E). The ratio of *amoA* to *nosZ-I* plus *nosZ-II* was higher in plantation soils than in Alan Batu, consistent with greater potential for N_2O accumulation. However, comparisons with other forest (Alan Bunga and Padang Alan) sites were limited because *amoA* was below detection at those sites (Fig. 5A–F).

3.5. *Biogeochemical drivers of N cycling and loss pathways across land uses*

The PCA revealed distinct biogeochemical patterns across the five land use types, with the first two principal components explaining 80.3% of the total variance (PC1: 63.6%; PC2: 16.7%; Fig. 6A). PC1, indicated by left and right pointing loading vectors (arrows), primarily reflected a gradient in soil O_2 availability, N transformation processes, and DIN leaching rates. Oil palm sites, which were positioned on the far right of this PCA, were characterized by higher soil O_2 concentrations, NO_3-N concentrations, GNR, field N_2O fluxes, DIN leaching rates, and enriched bulk soil $\delta^{15}N$. Based on their proximity and the direction of their loading vectors, these six variables were also positively correlated (Fig. 6A). In contrast, the forested sites positioned on the left side of PC1 exhibited higher soil NH_4-N concentrations, SWC, and GAR, as well as greater gene abundances of denitrifiers and N-fixers. From their loading vectors, these parameters were positively related to each other but negatively associated with the parameters on the far right of PC1 (Fig. 6A). PC2 primarily separated sites based on functional microbial groups, with three forested sites primarily occupying this space (Fig. 6A). Overall, the tight clustering of oil palm sites in the positive PC1 space contrasted markedly with the more dispersed distribution of natural peatland forest land uses (Alan Batu, Alan Bunga, Mixed peat swamp, and Padang Alan), which clustered mainly in the negative PC1 space (Fig. 6A).

Further bivariate analysis of these parameters also revealed apparent differences across the five land uses (Fig. 6B,C,D,E,F,G). Specifically, a decrease in SWC led to significant increases in the GNR:GAR, as well as similar increases in soil O_2 concentrations, along land use gradients from forested sites to oil palm sites (Fig. 6B). These increases in soil O_2 concentration and the GNR: GAR ratio also coincided with declines in the gene abundances of denitrifiers and N fixers (Fig. 6B–D). The in-vitro GNR:GAR ratios were also significantly positively related to the field-measured NO_3:NH_4 ratio and N_2O fluxes, which were highest at the oil palm sites (Fig. 6E). Bulk soil $\delta^{15}N$ isotopic enrichment showed a similar positive correlation with the field NO_3:NH_4 ratio, annual DIN leaching rates, and N_2O fluxes along a land use gradient from forested sites to oil palm sites (Fig. 6D and E).

4. Discussion

Conversion of tropical peat swamp forest to oil palm plantation is widely associated with increased N_2O emissions and higher NO_3-N leaching (Melling et al., 2007; Pardon et al., 2016b; Cooper et al., 2020; Formaglio et al., 2020; Midot et al., 2025). However, relatively few studies have identified the process-level mechanisms linking drainage and fertilization to these N losses in tropical peatland soils (e.g., Allen et al., 2015; Midot et al., 2025). By combining field measurements of N_2O fluxes and annual DIN leaching with process-based measurements of N cycling, mechanistic pathways that explains why converted peatlands act as persistent N-loss hotspots were identified. Specifically, drainage reduced soil water content and increased topsoil O_2 availability in the oil palm plantation, shifting soils from persistently reducing conditions toward more aerobic regimes (Dickopp et al., 2018; Ma et al., 2022). This redox transition, along with fertilizer-derived mineral N inputs, altered microbial N transformation processes. Plantation soils were characterized by nitrification-dominated turnover (high GNR and elevated GNR:GAR), increased nitrifier gene abundances, and decreased denitrifier gene abundances compared to forest sites. This shift promoted NO_3-N accumulation and mobility, increasing both N_2O emissions (Pärn et al., 2018) and DIN leaching (Pardon et al., 2016b). Enhanced nitrification, leaching, and gaseous N loss rates were

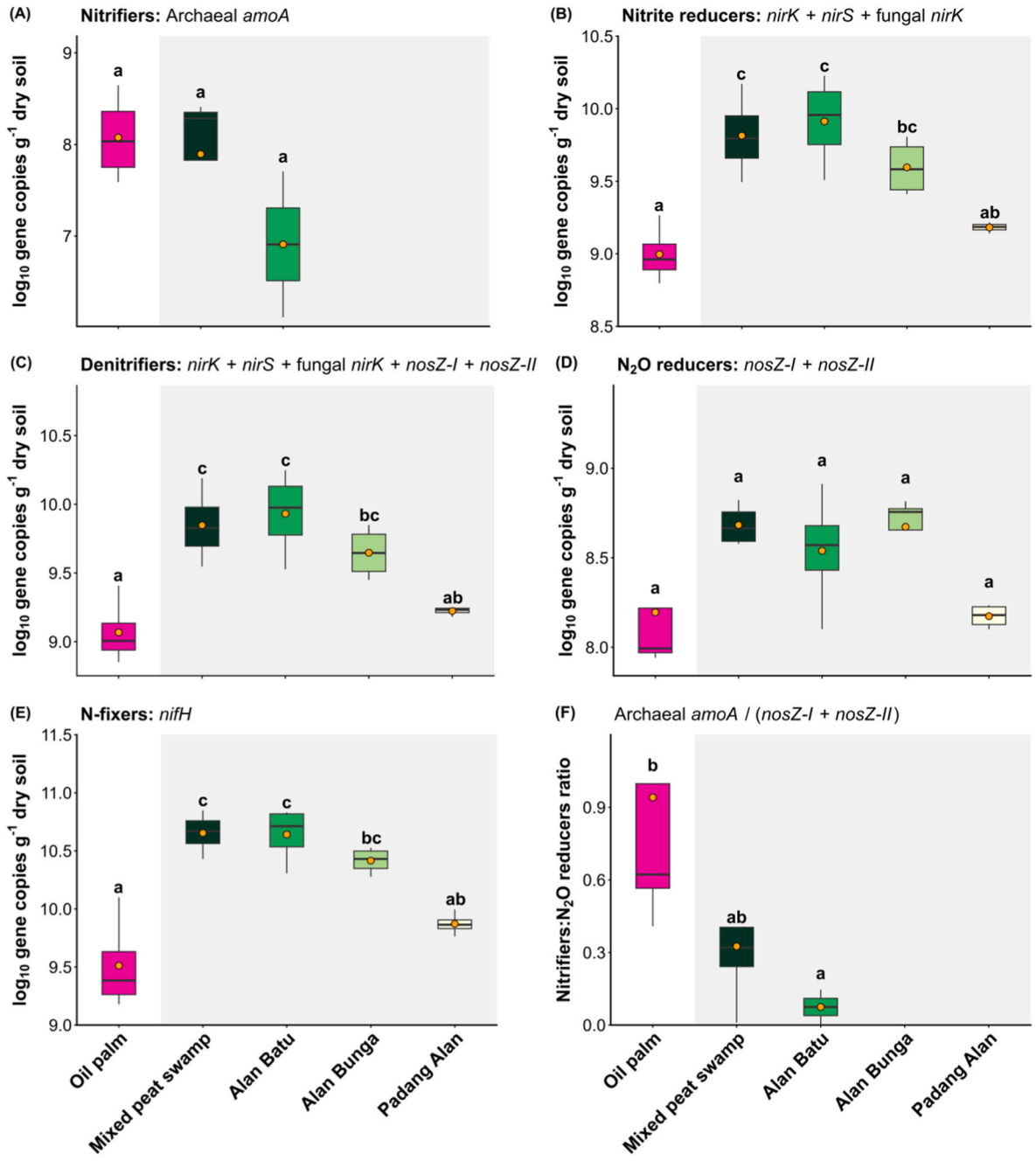

Fig. 5. Log-transformed abundances of microbial functional genes involved in N cycling across oil palm plantation and forest sites. Different lowercase letters above the boxplots indicate significant differences among sites (Kruskal–Wallis test followed by Dunn's post hoc test; $P < 0.05$). Archaeal *amoA* abundances at Alan Bunga and Padang Alan were below detection limits.

associated with more enriched bulk soil $\delta^{15}N$ signals in oil palm plantations relative to intact forest sites, suggesting that land use conversion promotes a more open N cycle. Overall, these findings suggest that bulk soil $\delta^{15}N$ patterns may serve as indicators of persistent intensified N inputs, N cycling, and losses in tropical peatlands under human-driven land use changes, in line with observations from other ecosystems (Craine et al., 2015a; Gerschlauer et al., 2019; Choi et al., 2020; Wangari et al., 2024).

4.1. Effects of land use on microbial-mediated N transformation rates

N_2O fluxes (−9.7 to 2405 μg-N m^{-2} h^{-1}) quantified in October 2024 fell within the range of those reported for converted and intact tropical peatland ecosystems (Liengaard et al., 2013; Mori, 2023; Midot et al., 2025). However, average fluxes varied significantly by land use, with plantation sites emitting several orders of magnitude more N_2O than forested soils, which were primarily weak N_2O sinks (Fig. 2). The peak N_2O flux (2405 μg N m^{-2} h^{-1}) observed at the plantation sites also represented one of the highest N_2O fluxes ever recorded for tropical peat soils, emphasizing the significance of these ecosystems as hotspots of N_2O within tropical peatlands (e.g., Jovani-Sancho et al., 2023; Mori, 2023). Converting peat forests into oil palm plantations involves various land management practices, including peat drainage to lower water tables and the application of synthetic N fertilizer. These management practices have been linked to elevated N_2O emissions in oil palm plantations due to shifts in redox conditions and soil N availability, which alter the balance between microbial production and consumption of N_2O (e.g., Melling et al., 2007; Mori, 2023). Nonetheless, few studies

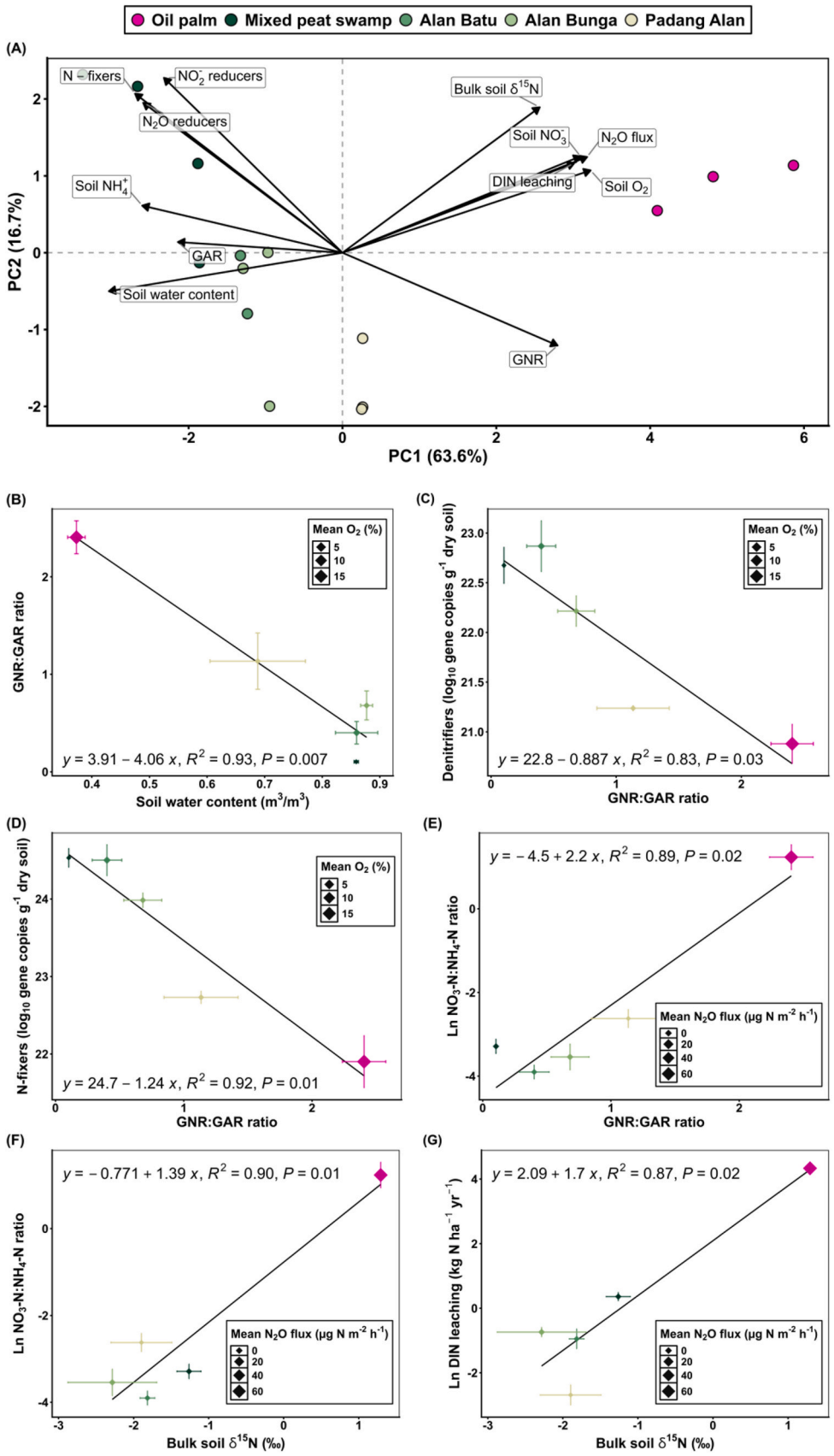

(caption on next page)

Fig. 6. (A) Principal component analysis of soil physico-chemical parameters, N_2O fluxes, N transformations rates, annual DIN leaching, and gene abundances across the oil palm and forest sites. Bivariate linear regressions between: (B) soil water content and GNR:GAR ratio (point size indicates soil O_2); (C) GNR:GAR ratios and denitrifier (*nirS, nirK, fungal nirK, nosZ-I, nosZ-II*) gene abundances (point size indicates soil O_2); (D) gross nitrification: ammonification ratios and N-fixers (*nifH*) gene abundances (point size indicates soil O_2); (E) GNR:GAR ratio and field-measured soil NO_3:NH_4 ratios (point size indicates N_2O fluxes); (F) bulk soil $\delta^{15}N$ and soil NO_3:NH_4 ratios (point size indicates N_2O fluxes); (G) bulk soil $\delta^{15}N$ and annual DIN leaching rates (point size indicates N_2O fluxes). Points and error bars represent means ± SE.

have directly explored the underlying processes within tropical peatland ecosystems (Skiba et al., 2020). The experimental work in this study aimed to address this gap by establishing linkages among field-based N_2O measurements, N cycling processes, and the gene abundances of the functional microbial groups involved.

From observations, peat drainage seemed to fundamentally alter soil redox conditions (e.g., Ma et al., 2022; Koskinen et al., 2025), as topsoil O_2 concentrations showed a negative relationship with SWC and were two orders of magnitude higher in the plantation sites than in the intact peat forests (Table S1; Fig. 6). Such exposure of peat soil microbes to higher O_2 concentrations has been shown to alter the rates of key N cycling processes (e.g., Pal et al., 2010). This agrees with the findings of this study, as the balance between GNR and GAR (Fig. 3) showed the most significant changes in response to redox alteration, suggesting that it is one of the driving factors behind the higher N_2O fluxes from plantation sites compared to intact forested sites.

Similar to N_2O fluxes, the range of GNR and GAR in this study (0.22 to 3.9 $\mu g\ N\ g^{-1}\ d^{-1}$) aligns with values reported for other terrestrial ecosystems (e.g., Wang et al., 2018; Gil et al., 2022; Ramm et al., 2022). However, direct comparison with gross N transformation estimates from other tropical peatlands, whether intact or converted, was challenging because this study is among the first to report such estimates for these ecosystems. Nonetheless, the up to 14.8 times higher GNR and consistently higher GNR:GAR ratios at drained oil palm sites than at forest sites (Fig. 3) coincided with higher soil O_2 concentrations measured at the plantation sites, suggesting that elevated O_2 availability may have promoted nitrification (Stenstrom and Poduska, 1980). This link between higher GNR:GAR ratios and increased O_2 levels was further supported by a positive correlation between the two parameters, which explained differences in rates across sites (Fig. 6).

While GNR were either equal to or lower than GAR at the forested sites, contrary patterns were observed at the plantation sites. Specifically, GNR were up to 186% higher than the respective GAR, suggesting that some of the NH_4-N converted to NO_3-N was externally sourced rather than internally produced. The application of urea-based fertilizer, characteristic of these plantations, may explain the availability of this excess N, similar to what was suggested in other studies (Melling et al., 2007; Shi et al., 2021). Beyond the effects of peat drainage on soil O_2 concentrations and peat mineralization (Hergoualc'h et al., 2017; Ma et al., 2022), these results directly link changes in N cycling rates to anthropogenic fertilization, providing mechanistic insights into how both practices (peat drainage and fertilization) simultaneously alter N cycling in converted tropical peatlands.

In addition to quantifying gross nitrification and ammonification rates, this study also examined denitrification products under varying O_2 concentrations (Fig. 4). At ambient O_2 levels, total denitrification (N_2+N_2O) rates showed no differences across land uses, contrary to our expectation of higher denitrification rates in oil palm plantations due to elevated NO_3 concentrations. However, apparent land use differences emerged when O_2 concentrations were experimentally reduced (Fig. 4). At very low O_2 levels, similar to those measured at forest sites, both N_2 and N_2O fluxes were up to two orders of magnitude higher in plantation soils than in forest soils, which had zero-to-negative fluxes for both gases. These low-to-negative N_2O fluxes at forest sites matched those measured in the field (Fig. 2) and also agreed with the high N fixation potential inferred from the high abundance of the *nifH* gene at these sites relative to the plantation sites (Fig. 5).

Similar to N_2O, the N_2O: (N_2O + N_2) product ratio also increased as O_2 concentrations declined from 20% to 10% in plantation soils, reaching up to 59% of total denitrification rates (Fig. 4). These results indicated that plantation soils may have a higher potential for N_2O production than forest soils even under reducing conditions. Such reducing conditions are likely to occur during heavy precipitation events, when rising soil water levels lower soil O_2 availability, potentially creating hot moments of N_2O emission. Similar precipitation-driven N_2O peaks have been reported in other tropical terrestrial ecosystems and were linked to altered soil redox conditions (Butterbach-Bahl et al., 2004; Midot et al., 2025). The contrasting experimental outcomes of denitrification under ambient and low O_2 conditions also highlight the need to conduct experiments that closely mimic in-situ conditions to obtain more accurate estimates of flux magnitudes and site differences. For instance, assuming N_2O production in the plantation originates from 0 to 20 cm peat soil depths, this scales in vitro N_2O fluxes under in-situ measured O_2 concentrations (15-5%) to a range of 160 to 500 $\mu g\ N\ m^{-2}\ h^{-1}$, which is consistent with the magnitudes quantified in the field (Table S1, Fig. S3).

Land use differences in N turnover rates were also reflected in the gene abundances of functional microbial groups responsible for key N cycling processes, as well as the field-measured DIN pools. For example, higher abundances of ammonium-oxidizing genes and lower abundances of denitrifier and N-fixer genes were observed at the oil-palm plantation sites compared with the intact forest sites (Fig. 5). This pattern may indicate that higher soil O_2 concentrations and increased NO_3-N availability in the oil palm plantation soils likely increased their nitrification potential and decreased their denitrification and N-fixation potential, consistent with past studies (Espenberg et al., 2018; Bahram et al., 2022). Moreover, the soil NO_3:NH_4 ratio scaled well with spatial differences in N_2O fluxes (Fig. 6), suggesting increased N_2O production via NO_3 reduction through the denitrification process (Butterbach-Bahl et al., 2013).

Consistent with patterns observed for N_2O fluxes and N turnover rates, average annual NH_4-N and NO_3-N leaching rates at oil palm plantation sites (89 $kg\ N\ ha^{-1}\ yr^{-1}$) substantially exceeded (by up to two orders of magnitude; Fig. 2) those quantified at the peat forest sites. The average NH_4-N and NO_3-N leaching rates across all land uses (0.1 to 89 $kg\ N\ ha^{-1}\ yr^{-1}$) in this study were within the ranges of those reported in previous field measurements and modelling studies in tropical regions (e.g., Formaglio et al., 2020; Pardon et al., 2016b). While NO_3-N accounted for the majority (>80%) of DIN leaching losses, substantial NH_4-N leaching was also observed at some oil palm plantation sites, with annual rates exceeding 50 $kg\ N\ ha^{-1}\ yr^{-1}$. These findings suggest that a portion of the applied ammonium-based fertilizers may have been directly lost through tile drainage in the acidic peat soils with low cation exchange capacity and subsequently captured by the resins.

4.2. Linking soil $\delta^{15}N$ with N cycling and losses across different land uses

Previous studies have linked soil $\delta^{15}N$ enrichment, which is also reflected in plant tissue, to more open N cycles characterized by elevated N inputs, cycling, and losses (Craine et al., 2009; Craine, et al., 2015a, 2015b; Wangari et al., 2024). Similar mechanisms likely explain the observed differences across land uses in this study, in which foliar and soil bulk $\delta^{15}N$ values were up to 3.36‰ more enriched at the plantation sites than at forest sites (Fig. S2). The link between land use-driven isotopic enrichment and accelerated N turnover was supported by the significant positive correlations we found between bulk soil $\delta^{15}N$ and

gross nitrification rates, N_2O fluxes, and total DIN leaching rates (Fig. 6). Such processes have been previously shown to enrich the residual soil N pool with the heavier ^{15}N isotope, as the lighter ^{14}N isotope is preferably cycled and lost to the environment (e.g., Craine et al., 2015b; Denk et al., 2017). Since bulk soil $\delta^{15}N$ integrates N dynamics over extended periods (Craine et al., 2015b), its positive correlation with recently elevated N cycling, gaseous, and hydrological loss rates at the oil palm sites in this study suggests that these hot spots may have persisted for prolonged periods. This finding aligns with conclusions from a previous temperate study (e.g., Wangari et al., 2024), but is the first to demonstrate this in converted tropical peatland ecosystems.

In addition to reflecting high N cycling and loss rates, bulk soil $\delta^{15}N$ signals may also be influenced by differences in N sources (Choi et al., 2020). For example, plant-soil $\delta^{15}N$ at the forest sites was mainly depleted in the heavier ^{15}N isotopes, suggesting N inputs primarily from the fixation of atmospheric nitrogen (Denk et al., 2017). Supporting this hypothesis, forest sites also had the highest potential for N-fixation, reflected by a higher abundance of the *nifH* gene relative to the oil palm plantation sites (Fig. 5; Fig. S4). The effects of differences in N sources may also have affected the soil $\delta^{15}N$ signals at the oil palm sites, as mineral N fertilizers, known to have near-zero $\delta^{15}N$ signals (Choi et al., 2020), may have diluted the enriched soil $\delta^{15}N$ signals at these sites.

4.3. Global relevance of the study

Oil palm cultivation on tropical peatlands is expected to remain a major land use pressure in Southeast Asia, with projections indicating continued expansion under business-as-usual scenarios (Leijten et al., 2023). The results in this study identify a mechanistic sequence that explains how conversion alters peatland N cycling, whereby drainage increases O_2 availability, fertilization increases mineral N supply, nitrification becomes dominant, NO_3-N accumulates, and hydrological and gaseous N losses intensify. This framework helps interpret spatial heterogeneity in N losses within peat landscapes and supports bulk soil $\delta^{15}N$ as a diagnostic indicator of long-term anthropogenic disturbance effects on peatland N cycling. Here, a simplified N balance was developed to quantify anthropogenic effects on peatland N cycles by synthesizing regional estimates of primary N inputs, plant N uptake (Pardon et al., 2016b), and, for the first time, field-based measurements of N leaching and estimates of N_2 emissions from denitrification ratios (Fig. 7). The analysis revealed that combined hydrological and gaseous N losses exceed oil palm N uptake, indicating a fundamentally open N cycle within oil palm plantations that contrasts sharply with the natural peatland forest ecosystems, which show no significant N losses (Fig. 7).

To validate the net N losses quantified in this study, the values were compared with the reported net C losses in the literature using the quantified C: N ratios in this study (Fig. 2). Under oil palm cultivation on peat, the strongly negative net N balance corresponded to an implied soil C loss of 3.7 ± 4.8 Mg C ha^{-1} yr^{-1} (C: N = 28), whereas intact peat forests showed a much smaller net N deficit, translating to an implied soil C loss of 0.4 ± 0.4 Mg C ha^{-1} yr^{-1} based on a C: N ratio of 33. Despite the existing uncertainties within the N balance, these values were of the same order of magnitude as those reported for C losses in forests (2.0 ± 0.9 Mg C ha^{-1} yr^{-1}) and oil palm plantations (4.9 ± 1.2 Mg C ha^{-1} yr^{-1}) in other studies within Southeast Asia (Hergoualc'h et al., 2017). The implied C losses in the oil palm plantation sites were also within the same order of magnitude, albeit on the lower end compared with the default IPCC emission factor for oil palm plantations on peat of 11.8 (6.2 - 18.1) Mg C ha^{-1} yr^{-1} (Drösler et al., 2014), cumulatively suggesting that the quantified N losses match previously quantified C losses. These estimates also show that oil palm conversion fundamentally disrupts coupled carbon–nitrogen dynamics in tropical peatlands, leading to substantially greater C and N losses from existing peat stocks than in intact forests.

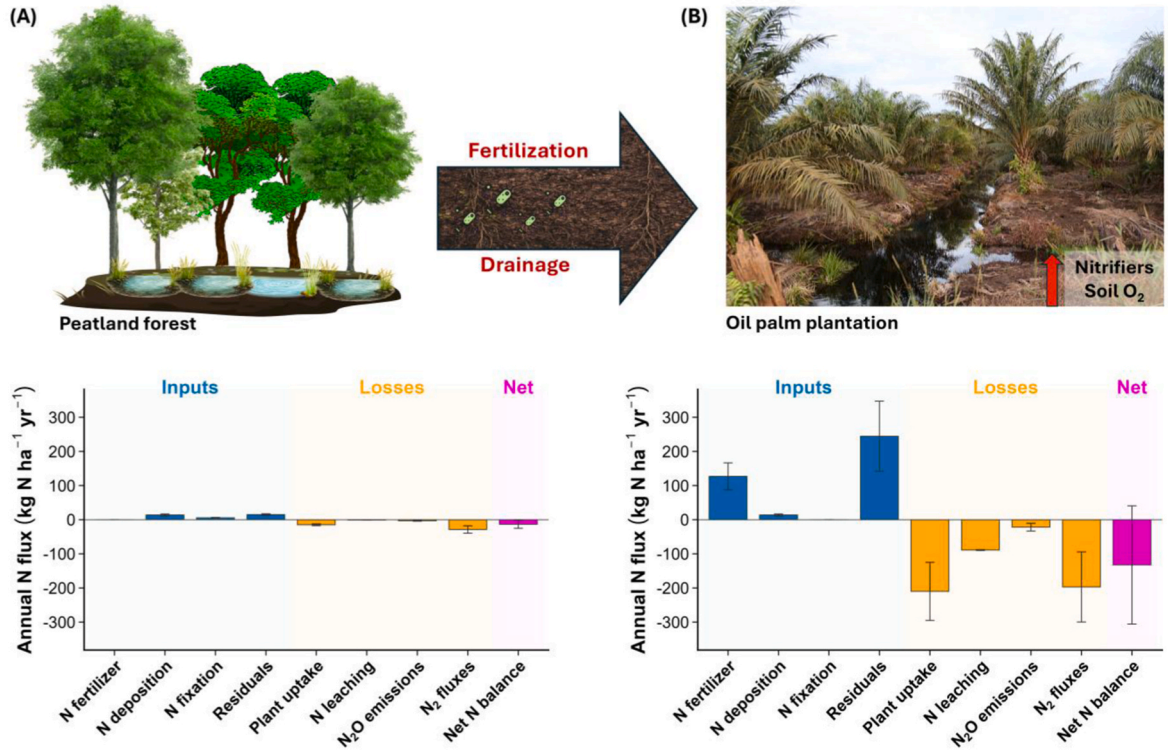

Fig. 7. Conceptual summary of land use effects on N cycling and a simplified N balance for intact peat swamp forest and oil palm plantation. The N balance includes regional estimates (annual mean ± SE; assuming normal distributions bounded by reported minimum and maximum values) for mineral fertilizer inputs, atmospheric N deposition, residual inputs, and plant N uptake from Pardon et al. (2016a); annual N_2O estimates from Jovani-Sancho et al. (2023); and N_2 losses and annual DIN leaching from this study (with N_2 estimated using the denitrification product ratio of 0.1). Net N balance is calculated as total N inputs (blue) minus total N outputs.

4.4. Limitations of the study

Despite the insights gained in this study, several limitations should be considered when interpreting its findings. For example, leaching rates in this study only provided cumulative annual estimates, whereas most other components of N transformation and loss rates, including N_2O and N_2 fluxes and gross nitrification and ammonification rates, were derived from snapshot measurements. Consequently, these observations likely missed important temporal "hot moments," particularly for DIN leaching and process rates, which remain poorly constrained over longer temporal time scales compared to N_2O fluxes, which are well represented by extensive regional datasets (Jovani-Sancho et al., 2023). The helium incubation experiment examining effects of O_2 levels was carried out over several days, thus the observed changes in N_2 and N_2O fluxes may also be due to changes in substrate availability over time. Further methodological limitations arise from the temporal mismatch between the field-based N_2O flux measurements and laboratory analyses of N transformation and loss rates due to technical constraints.

Addressing these gaps will require future studies to prioritize paired, high-resolution time-series measurements of biogeochemical process rates alongside hydrological and gaseous N losses to better resolve the temporal controls governing N export. This study was also not a strictly controlled experiment, thus the observed N transformation and loss rates may have also been influenced by other unaccounted factors such as variability in mineral fertilizer inputs and differences in plant traits and vegetation types (e.g., Zhang et al., 2024). In addition, the components of the simplified N balance are subject to substantial uncertainty, as individual fluxes exhibit pronounced spatial variability. Further work aimed at constraining these individual terms is therefore essential to improve confidence in integrated N balance estimates for the tropical peatland ecosystems.

5. Conclusions

This study shows that differences in N_2O fluxes and N leaching between intact peat swamp forests and oil palm plantations are primarily driven by increases in soil O_2 availability and synthetic fertilizer inputs, which together alter key N cycling processes. In the plantation, increased soil aeration and fertilizer-derived N promoted nitrification-dominated turnover, as indicated by gross nitrification rates exceeding gross ammonification and by higher abundance of nitrification-associated genes. These changes led to greater accumulation of soil NO_3-N and were accompanied by substantially higher NO_3-N leaching losses. These findings highlight the environmental consequences of converting tropical peatlands, including increased emissions of potent GHG and surface-water contamination from reactive N export. Bulk soil $\delta^{15}N$ enrichment in plantation soils further suggested that the sites had sustained higher N inputs, N cycling, and losses, reflecting a more open N cycle. In contrast, intact peat forest sites maintained a conservative N cycling, with low N_2O fluxes and DIN leaching losses. Together, these findings indicate substantial potential for mitigating climate change and improving water quality through management strategies that prioritize protecting intact peat swamp forests and restoring or rewetting degraded peatlands, along with improved fertilizer management to reduce N losses.

Funding sources

This research was funded by the Estonian Research Agency (grant number PRG2032), Estonian Ministry of Education and Research, Centre of Excellence for Agroecology and New Crops in Future Climates (TK200), by the European Union (ERC AdG PeatlandN2O, 101096403), European Union Horizon program (LiWeFor, 101079192), and Pioneer Center for Landscape Research in Sustainable Agricultural Futures (Land-CRAFT), DNRF grant number P2. Part of the research infrastructure was provided by the Helmholtz Association through the joint program Changing Earth – Sustaining our Future (ATMO - PoF IV) program of Karlsruhe Institute of Technology (KIT).

CRediT authorship contribution statement

Elizabeth Gachibu Wangari: Conceptualization, Data curation, Formal analysis, Visualization, Writing – original draft, Writing – review & editing. **Kien Yung Teo:** Data curation, Formal analysis, Writing – review & editing. **Ricky Mwangada Mwanake:** Data curation, Formal analysis, Writing – review & editing. **Faustina Elfrida Sangok:** Data curation, Writing – review & editing. **Herman Umbau Lindang:** Data curation, Writing – review & editing. **Auldry Chaddy:** Data curation, Writing – review & editing. **Sharon Yu Ling Lau:** Data curation, Writing – review & editing. **Fawad Khan:** Data curation, Writing – review & editing. **Nur Azima Busman:** Data curation, Writing – review & editing. **Kim San Lo:** Data curation, Writing – review & editing. **Hanna Vahter:** Data curation, Writing – review & editing. **Muhammad Kamil-Sardar:** Data curation, Writing – review & editing. **Kärt Kanger:** Data curation, Writing – review & editing. **Georg Willibald:** Data curation, Writing – review & editing. **Per Ambus:** Data curation, Writing – review & editing. **Mari Pihlatie:** Funding acquisition, Writing – review & editing. **Kaido Soosaar:** Conceptualization, Data curation, Funding acquisition, Writing – review & editing. **Mikk Espenberg:** Conceptualization, Data curation, Funding acquisition, Writing – review & editing. **Klaus Butterbach-Bahl:** Conceptualization, Data curation, Funding acquisition, Writing – review & editing. **Ralf Kiese:** Conceptualization, Data curation, Funding acquisition, Writing – review & editing. **Ülo Mander:** Conceptualization, Data curation, Funding acquisition, Writing – review & editing. **Lulie Melling:** Conceptualization, Data curation, Funding acquisition, Writing – review & editing.

Declaration of competing interest

The authors declare that they have no known competing financial interests or personal relationships that could have appeared to influence the work reported in this paper.

Acknowledgements

The authors would like to express their sincere gratitude to the staff of the Sarawak Tropical Peat Research Institute for their invaluable logistical support and assistance with fieldwork and sample analyses.

Appendix A. Supplementary data

Supplementary data to this article can be found online at https://doi.org/10.1016/j.jenvman.2026.130427.

Data availability

Data will be made available on request.

References

Allen, K., Corre, M.D., Tjoa, A., Veldkamp, E., 2015. Soil nitrogen-cycling responses to conversion of lowland forests to oil palm and rubber plantations in Sumatra, Indonesia. PLoS One 10 (7), e0133325. https://doi.org/10.1371/journal.pone.0133325.

Anderson, J.A.R., 1963. The Flora of the peat swamp forests of Sarawak and Brunei, including a catalogue of all recorded species of flowering plants. Ferns and Fern Allies.

Bahram, M., Espenberg, M., Pärn, J., Lehtovirta-Morley, L., Anslan, S., Kasak, K., Kõljalg, U., Liira, J., Maddison, M., Moora, M., Niinemets, Ü., Öpik, M., Pärtel, M., Soosaar, K., Zobel, M., Hildebrand, F., Tedersoo, L., Mander, Ü., 2022. Structure and function of the soil microbiome underlying N_2O emissions from global wetlands. Nat. Commun. 13 (1), 1430. https://doi.org/10.1038/s41467-022-29161-3.

Bai, E., Houlton, B.Z., Wang, Y.P., 2012. Isotopic identification of nitrogen hotspots across natural terrestrial ecosystems. Biogeosciences 9 (8), 3287–3304. https://doi.org/10.5194/bg-9-3287-2012.

Baumgartner, S., Bauters, M., Barthel, M., Drake, T.W., Ntaboba, L.C., Bazirake, B.M., Six, J., Boeckx, P., Van Oost, K., 2021. Stable isotope signatures of soil nitrogen on an environmental–geomorphic gradient within the Congo Basin. SOIL 7 (1), 83–94. https://doi.org/10.5194/soil-7-83-2021.

Bolleter, W.T., Bushman, C.J., Tidwell, P.W., 1961. Spectrophotometric Determination of Ammonia as Indophenol.

Braun, J., Mooshammer, M., Wanek, W., Prommer, J., Walker, T.W.N., Rütting, T., Richter, A., 2018. Full 15N tracer accounting to revisit major assumptions of ^{15}N isotope pool dilution approaches for gross nitrogen mineralization. Soil Biol. Biochem. 117, 16–26. https://doi.org/10.1016/j.soilbio.2017.11.005.

Butterbach-Bahl, K., Baggs, E.M., Dannenmann, M., Kiese, R., Zechmeister-Boltenstern, S., 2013. Nitrous oxide emissions from soils: how well do we understand the processes and their controls? Phil. Trans. Biol. Sci. 368 (1621), 20130122. https://doi.org/10.1098/rstb.2013.0122.

Butterbach-Bahl, K., Willibald, G., Papen, H., 2002. Soil core method for direct simultaneous determination of N_2 and N_2O emissions from forest soils. Plant Soil 240 (1), 105–116. https://doi.org/10.1023/A:1015870518723.

Butterbach-Bahl, K., Kock, M., Willibald, G., Hewett, B., Buhagiar, S., Papen, H., Kiese, R., 2004. Temporal variations of fluxes of NO, NO_2 , N_2O, CO_2 , and CH_4 in a tropical rain forest ecosystem. Glob. Biogeochem. Cycles 18 (3). https://doi.org/10.1029/2004GB002243.

Byun, E., Müller, C., Parisse, B., Napoli, R., Zhang, J.-B., Rezanezhad, F., Van Cappellen, P., Moser, G., Jansen-Willems, A.B., Yang, W.H., Urakawa, R., Arroyo, J. I., Neri, U., Elrys, A.S., Nardi, P., 2024. A global dataset of gross nitrogen transformation rates across terrestrial ecosystems. Sci. Data 11 (1), 1022. https://doi.org/10.1038/s41597-024-03871-3.

Chen, G., Liu, C., Li, Z., Zhang, B., Zhou, G., Lin, Y., Wang, J., Wang, X., Ye, J., Zhang, H., Wu, Z., Xiao, H., 2024. Large contribution of soil N_2O emission to the global warming effect of greenhouse gases in vegetable fields. Biogeosciences 21 (2), 513–527. https://doi.org/10.5194/bg-21-513-2024.

Choi, W.-J., Kwak, J.-H., Park, H.-J., Yang, H., Park, S.-I., Xu, Z., Lee, S.-M., Lim, S.-S., Chang, S.X., 2020. Land-use type, and land management and disturbance affect soil $\delta^{15}N$: a review. J. Soils Sediments 20 (9), 3283–3299. https://doi.org/10.1007/s11368-020-02708-x.

Comeau, L.-P., Hergoualc'h, K., Hartill, J., Smith, J., Verchot, L.V., Peak, D., Salim, A.M., 2016. How do the heterotrophic and the total soil respiration of an oil palm plantation on peat respond to nitrogen fertilizer application? Geoderma 268, 41–51. https://doi.org/10.1016/j.geoderma.2016.01.016.

Cooper, H.V., Evers, S., Aplin, P., Crout, N., Dahalan, M. P. Bin, Sjogersten, S., 2020. Greenhouse gas emissions resulting from conversion of peat swamp forest to oil palm plantation. Nat. Commun. 11 (1), 407. https://doi.org/10.1038/s41467-020-14298-w.

Craine, J.M., Brookshire, E.N.J., Cramer, M.D., Hasselquist, N.J., Koba, K., Marin-Spiotta, E., Wang, L., 2015b. Ecological interpretations of nitrogen isotope ratios of terrestrial plants and soils. Plant Soil 396 (1–2), 1–26. https://doi.org/10.1007/s11104-015-2542-1.

Craine, J.M., Elmore, A.J., Aidar, M.P.M., Bustamante, M., Dawson, T.E., Hobbie, E.A., Kahmen, A., Mack, M.C., McLauchlan, K.K., Michelsen, A., Nardoto, G.B., Pardo, L. H., Peñuelas, J., Reich, P.B., Schuur, E.A.G., Stock, W.D., Templer, P.H., Virginia, R. A., Welker, J.M., Wright, I.J., 2009. Global patterns of foliar nitrogen isotopes and their relationships with climate, mycorrhizal fungi, foliar nutrient concentrations, and nitrogen availability. New Phytol. 183 (4), 980–992. https://doi.org/10.1111/j.1469-8137.2009.02917.x.

Craine, J.M., Elmore, A.J., Wang, L., Augusto, L., Baisden, W.T., Brookshire, E.N.J., Cramer, M.D., Hasselquist, N.J., Hobbie, E.A., Kahmen, A., Koba, K., Kranabetter, J. M., Mack, M.C., Marin-Spiotta, E., Mayor, J.R., McLauchlan, K.K., Michelsen, A., Nardoto, G.B., Oliveira, R.S., et al., 2015a. Convergence of soil nitrogen isotopes across global climate gradients. Sci. Rep. 5 (1), 8280. https://doi.org/10.1038/srep08280.

Denk, T.R.A., Mohn, J., Decock, C., Lewicka-Szczebak, D., Harris, E., Butterbach-Bahl, K., Kiese, R., Wolf, B., 2017. The nitrogen cycle: a review of isotope effects and isotope modeling approaches. Soil Biol. Biochem. 105, 121–137. https://doi.org/10.1016/j.soilbio.2016.11.015.

Dickopp, J., Lengerer, A., Kazda, M., 2018. Relationship between groundwater levels and oxygen availability in fen peat soils. Ecol. Eng. 120, 85–93. https://doi.org/10.1016/j.ecoleng.2018.05.033.

Dijkstra, P., Ishizu, A., Doucett, R., Hart, S.C., Schwartz, E., Menyailo, O.V., Hungate, B. A., 2006. ^{13}C and ^{15}N natural abundance of the soil microbial biomass. Soil Biol. Biochem. 38 (11), 3257–3266. https://doi.org/10.1016/j.soilbio.2006.04.005.

Drösler, M., Verchot, L.V., Freibauer, A., Pan, G., Evans, C.D., Bourbonniere, R.A., Alm, J. P., Page, S., Agus, F., Hergoualc'h, K., Couwenberg, J., Jauhiainen, J., Sabiham, S., Wang, C., Srivastava, N., Borgeau-Chavez, L., Hooijer, A., et al., 2014. Chapter 2: Drained inland organic soils. In: Hiraishi, T., Krug, T., Tanabe, K., Srivastava, N., Jamsranjav, B., Fukuda, M., Troxler, T. (Eds.), 2013 Supplement to the 2006 Guidelines for National Greenhouse Gas Inventories: Wetlands. IPCC, Geneva.

Emmett, B.A., Kjønaas, O.J., Gundersen, P., Koopmans, C., Tietema, A., Sleep, D., 1998. Natural abundance of ^{15}N in forests across a nitrogen deposition gradient. For. Ecol. Manag. 101 (1–3), 9–18. https://doi.org/10.1016/S0378-1127(97)00121-7.

Espenberg, M., Pille, K., Yang, B., Maddison, M., Abdalla, M., Smith, P., Li, X., Chan, P.-L., Mander, Ü., 2024. Towards an integrated view on microbial CH_4, N_2O and N_2 cycles in brackish coastal marsh soils: a comparative analysis of two sites. Sci. Total Environ. 918, 170641. https://doi.org/10.1016/j.scitotenv.2024.170641.

Espenberg, M., Truu, M., Mander, Ü., Kasak, K., Nõlvak, H., Ligi, T., Oopkaup, K., Maddison, M., Truu, J., 2018. Differences in microbial community structure and nitrogen cycling in natural and drained tropical peatland soils. Sci. Rep. 8 (1), 4742. https://doi.org/10.1038/s41598-018-23032-y.

Figueiredo, V., Enrich-Prast, A., Rütting, T., 2019. Evolution of nitrogen cycling in regrowing Amazonian rainforest. Sci. Rep. 9 (1), 8538. https://doi.org/10.1038/s41598-019-43963-4.

Formaglio, G., Veldkamp, E., Duan, X., Tjoa, A., Corre, M.D., 2020. Herbicide weed control increases nutrient leaching compared to mechanical weeding in a large-scale oil palm plantation. Biogeosciences 17 (21), 5243–5262. https://doi.org/10.5194/bg-17-5243-2020.

Gerschlauer, F., Saiz, G., Schellenberger Costa, D., Kleyer, M., Dannenmann, M., Kiese, R., 2019. Stable carbon and nitrogen isotopic composition of leaves, litter, and soils of various ecosystems along an elevational and land-use gradient at Mount Kilimanjaro, Tanzania. Biogeosciences 16 (2), 409–424. https://doi.org/10.5194/bg-16-409-2019.

Gil, J., Marushchak, M.E., Rütting, T., Baggs, E.M., Pérez, T., Novakovskiy, A., Trubnikova, T., Kaverin, D., Martikainen, P.J., Biasi, C., 2022. Sources of nitrous oxide and the fate of mineral nitrogen in subarctic permafrost peat soils. Biogeosciences 19 (10), 2683–2698. https://doi.org/10.5194/bg-19-2683-2022.

Gütlein, A., Dannenmann, M., Kiese, R., 2016. Gross nitrogen turnover rates of a tropical lower montane forest soil: impacts of sample preparation and storage. Soil Biol. Biochem. 95, 8–10. https://doi.org/10.1016/j.soilbio.2015.12.002.

Gurmesa, G.A., Hobbie, E.A., Zhang, S., Wang, A., Zhu, F., Zhu, W., Koba, K., Yoh, M., Wang, C., Zhang, Q., Fang, Y., 2022. Natural ^{15}N abundance of ammonium and nitrate in soil profiles: New insighns into forest ecosystem nitrogen saturation. Ecosphere 13 (3). https://doi.org/10.1002/ecs2.3998.

Hatano, R., 2025. Impacts of changes in peat soils due to agricultural activities on greenhouse gas (especially N_2O) emissions and their mitigations. Pedosphere 35 (1), 8–11. https://doi.org/10.1016/j.pedsph.2023.12.010.

Hergoualc'h, K., Hendry, D.T., Murdiyarso, D., Verchot, L.V., 2017. Total and heterotrophic soil respiration in a swamp forest and oil palm plantations on peat in Central Kalimantan, Indonesia. Biogeochemistry 135 (3), 203–220. https://doi.org/10.1007/s10533-017-0363-4.

Hood-Nowotny, R., Umana, N.H.-N., Inselbacher, E., Oswald- Lachouani, P., Wanek, W., 2010. Alternative methods for measuring inorganic, organic, and total dissolved nitrogen in soil. Soil Sci. Soc. Am. J. 74 (3), 1018–1027. https://doi.org/10.2136/sssaj2009.0389.

Ishikura, K., Hirano, T., Okimoto, Y., Hirata, R., Kiew, F., Melling, L., Aeries, E.B., Lo, K. S., Musin, K.K., Waili, J.W., Wong, G.X., Ishii, Y., 2018. Soil carbon dioxide emissions due to oxidative peat decomposition in an oil palm plantation on tropical peat. Agric. Ecosyst. Environ. 254, 202–212. https://doi.org/10.1016/j.agee.2017.11.025.

Jovani-Sancho, A.J., O'Reilly, P., Anshari, G., Chong, X.Y., Crout, N., Evans, C.D., Evers, S., Gan, J.Y., Gibbins, C.N., Gusmayanti, E., Jamaludin, J., Jaya, A., Page, S., Yosep, Y., Upton, C., Wilson, P., Sjögersten, S., 2023. CH_4 and N_2O emissions from smallholder agricultural systems on tropical peatlands in southeast Asia. Glob. Change Biol. 29 (15), 4279–4297. https://doi.org/10.1111/gcb.16747.

Kana, T.M., Darkangelo, C., Hunt, M.D., Oldham, J.B., Bennett, G.E., Cornwell, J.C., 1994. Membrane inlet mass spectrometer for rapid high-precision determination of N_2, O_2, and Ar in environmental water samples. Anal. Chem. 66 (23), 4166–4170. https://doi.org/10.1021/ac00095a009.

Khan, F., Franco-Luesma, S., Dannenmann, M.U., Gasche, R., Gattinger, A., Hartmann, F., Tobisch, B., Kiese, R., Wolf, B., 2025. Integrated rather than organic farming history facilitates soil nitrogen turnover and N_2O reduction in a green rye – silage maize cropping sequence. Biol. Fertil. Soils 61 (1), 27–41. https://doi.org/10.1007/s00374-024-01865-2.

Kiew, F., Hirata, R., Hirano, T., Wong, G.X., Aeries, E.B., Musin, K.K., Waili, J.W., Lo, K. S., Shimizu, M., Melling, L., 2018. CO_2 balance of a secondary tropical peat swamp forest in Sarawak, Malaysia. Agric. For. Meteorol. 248, 494–501. https://doi.org/10.1016/j.agrformet.2017.10.022.

Koh, L.P., Miettinen, J., Liew, S.C., Ghazoul, J., 2011. Remotely sensed evidence of tropical peatland conversion to oil palm. Proc. Natl. Acad. Sci. 108 (12), 5127–5132. https://doi.org/10.1073/pnas.1018776108.

Koskinen, M., Anttila, J., Vranová, V., Holík, L., Roche, K., Vorenhout, M., Pihlatie, M., Laiho, R., 2025. Covariation of redox potential profiles and the water table level at peatland sites representing different drainage regimes: implications for ecological modelling. Biogeosciences 22 (15), 3989–4012. https://doi.org/10.5194/bg-22-3989-2025.

Lam, S.K., Goodrich, J.P., Liang, X., Zhang, Y., Pan, B., Schipper, L.A., Sulaeman, Y., Nelson, L., Chen, D., 2022. Mitigating soil greenhouse-gas emissions from land-use change in tropical peatlands. Front. Ecol. Environ. 20 (6), 352–360. https://doi.org/10.1002/fee.2497.

Leijten, F., Lantz C Baldos, U., Johnson, J.A., Sim, S., Verburg, P.H., 2023. Projecting global oil palm expansion under zero-deforestation commitments: direct and indirect land use change impacts. iScience 26 (6), 106971. https://doi.org/10.1016/j.isci.2023.106971.

Liengaard, L., Nielsen, L.P., Revsbech, N.P., Priemé, A., Elberling, B., Enrich-Prast, A., Kühl, M., 2013. Extreme emission of N_2O from tropical wetland soil (Pantanal, South America). Front. Microbiol. 3. https://doi.org/10.3389/fmicb.2012.00433.

Lin, X., Li, X., Gao, D., Liu, M., Cheng, L., 2017. Ammonium production and removal in the sediments of Shanghai River networks: spatiotemporal variations, controlling factors, and environmental implications. J. Geophys. Res. Biogeosci. 122 (10), 2461–2478. https://doi.org/10.1002/2017JG003769.

Ma, L., Zhu, G., Chen, B., Zhang, K., Niu, S., Wang, J., Ciais, P., Zuo, H., 2022. A globally robust relationship between water table decline, subsidence rate, and carbon release from peatlands. Commun. Earth Environ. 3 (1), 254. https://doi.org/10.1038/s43247-022-00590-8.

Mander, Ü., Espenberg, M., Öpik, M., Mu, X., Ni, J., Voigt, C., Gogo, S., 2024. Peatland restoration pathways to mitigate greenhouse gas emissions and retain peat carbon.

Biogeochemistry. https://doi.org/10.1007/s10533-023-01103-1. Advance online publication.
McCalmont, J., Kho, L.K., Teh, Y.A., Lewis, K., Chocholek, M., Rumpang, E., Hill, T., 2021. Short- and long-term carbon emissions from oil palm plantations converted from logged tropical peat swamp forest. Glob. Change Biol. 27 (11), 2361–2376. https://doi.org/10.1111/gcb.15544.
Melling, L., 2016. Peatland in Malaysia. In: Tropical Peatland Ecosystems. Springer, Japan, pp. 59–73. https://doi.org/10.1007/978-4-431-55681-7_4.
Melling, L., Hatano, R., Goh, K.J., 2007. Nitrous oxide emissions from three ecosystems in tropical peatland of Sarawak, Malaysia. Soil Sci. Plant Nutr. 53 (6), 792–805. https://doi.org/10.1111/j.1747-0765.2007.00196.x.
Melling, L., Tan, C.Y., Goh, K.J., Hatano, R., 2013. Soil microbial and root respirations from three ecosystems in tropical peatland of Sarawak, Malaysia. Journal of Oil Palm Research 25 (1), 44–57.
Midot, F., Goh, K.M., Liew, K.J., Lau, S.Y.L., Espenberg, M., Mander, Ü., Melling, L., 2025. Temporal dynamics of soil microbial C and N cycles with GHG fluxes in the transition from tropical peatland forest to oil palm plantation. Appl. Environ. Microbiol. 91 (1). https://doi.org/10.1128/aem.01986-24.
Monda, Y., Kiyono, Y., Chaddy, A., Damian, C., Melling, L., 2018. Association of growth and hollow stem development in Shorea albida trees in a tropical peat swamp forest in Sarawak, Malaysia. Trees (Berl.) 32 (5), 1357–1364. https://doi.org/10.1007/s00468-018-1717-9.
Mori, T., 2023. Effects of tropical forest conversion into oil palm plantations on nitrous oxide emissions: a meta-analysis. J. For. Res. 34 (3), 865–869. https://doi.org/10.1007/s11676-022-01493-2.
Murphy, D., Recous, S., Stockdale, E., Fillery, I.R., Jensen, L., Hatch, D., Goulding, K.W., 2003. Gross nitrogen fluxes in soil : theory, measurement and application of ^{15}N pool dilution techniques, 69–118. https://doi.org/10.1016/S0065-2113(02)79002-0.
Mwanake, R.M., Wangari, E.G., Kikowatz, H.-M., Allgaier, M., Kolar, A., Kiese, R., 2026. Natural abundance sediment $\delta^{15}N$ as a proxy for long-term gross N-turnover processes, GHG emissions, and denitrification hotspots within fluvial ecosystems. Environ. Adv. 100685. https://doi.org/10.1016/j.envadv.2026.100685.
Page, S.E., Rieley, J.O., Banks, C.J., 2011. Global and regional importance of the tropical peatland carbon pool. Glob. Change Biol. 17 (2), 798–818. https://doi.org/10.1111/j.1365-2486.2010.02279.x.
Pal, L., Stres, B., Danevčič, T., Leskovec, S., Mandic-Mulec, I., 2010. Transformations of mineral nitrogen applied to peat soil during sequential oxic/anoxic cycling. Soil Biol. Biochem. 42 (8), 1338–1346. https://doi.org/10.1016/j.soilbio.2010.03.013.
Pardo, L.H., Nadelhoffer, K.J., 2010. Using nitrogen isotope ratios to assess terrestrial ecosystems at regional and global scales. In: Isoscapes. Springer, Netherlands, pp. 221–249. https://doi.org/10.1007/978-90-481-3354-3_11.
Pardon, L., Bessou, C., Nelson, P.N., Dubos, B., Ollivier, J., Marichal, R., Caliman, J.-P., Gabrielle, B., 2016a. Key unknowns in nitrogen budget for oil palm plantations. A review. Agron. Sustain. Dev. 36 (1), 20. https://doi.org/10.1007/s13593-016-0353-2.
Pardon, L., Bessou, C., Saint-Geours, N., Gabrielle, B., Khasanah, N., Caliman, J.-P., Nelson, P.N., 2016b. Quantifying nitrogen losses in oil palm plantations: models and challenges. Biogeosciences 13 (19), 5433–5452. https://doi.org/10.5194/bg-13-5433-2016.
Pärn, J., Verhoeven, J.T.A., Butterbach-Bahl, K., Dise, N.B., Ullah, S., Aasa, A., Egorov, S., Espenberg, M., Järveoja, J., Jauhiainen, J., Kasak, K., Klemedtsson, L., Kull, A., Laggoun-Défarge, F., Lapshina, E.D., Lohila, A., Lõhmus, K., Maddison, M., Mitsch, W.J., et al., 2018. Nitrogen-rich organic soils under warm well-drained conditions are global nitrous oxide emission hotspots. Nat. Commun. 9 (1), 1135. https://doi.org/10.1038/s41467-018-03540-1.
R Core Team, 2025. R: a Language and Environment for Statistical Computing. R Foundation for Statistical Computing, Vienna, Austria. https://www.R-project.org/.
Ramm, E., Liu, C., Mueller, C.W., Gschwendtner, S., Yue, H., Wang, X., Bachmann, J., Bohnhoff, J.A., Ostler, U., Schloter, M., Rennenberg, H., Dannenmann, M., 2022. Alder-induced stimulation of soil gross nitrogen turnover in a permafrost-affected peatland of Northeast China. Soil Biol. Biochem. 172, 108757. https://doi.org/10.1016/j.soilbio.2022.108757.
Ratai, J., Teh, C.B.S., Tan, N.P., Mohidin, H., Goh, K.J., Sangok, F.E., Melling, L., 2024. Tropical peat soil changes across successive oil palm generations in Sarawak, Malaysia. Heliyon 10 (18), e37754. https://doi.org/10.1016/j.heliyon.2024.e37754.
Reiss, K., Mander, Ü., Öpik, M., Sepp, S.-K., Kanger, K., Schindler, T., Soosaar, K., Pihlatie, M., Butterbach-Bahl, K., Putkinen, A., Niinemets, Ü., Espenberg, M., 2025. Temporal and spatial dynamics of microbial communities and greenhouse gas flux responses to experimental flooding in riparian forest soils. FEMS (Fed. Eur. Microbiol. Soc.) Microbiol. Ecol. 101 (12). https://doi.org/10.1093/femsec/fiaf109.
Robinson, D., 2001. $\delta^{15}N$ as an integrator of the nitrogen cycle. Trends Ecol. Evol. 16 (3), 153–162. https://doi.org/10.1016/S0169-5347(00)02098-X.
Ruijter, J.M., Ramakers, C., Hoogaars, W.M.H., Karlen, Y., Bakker, O., van den Hoff, M.J.B., Moorman, A.F.M., 2009. Amplification efficiency: linking baseline and bias in the analysis of quantitative PCR data. Nucleic Acids Res. 37 (6), e45. https://doi.org/10.1093/nar/gkp045 e45.
Sheng, W., Yu, G., Fang, H., Liu, Y., Wang, Q., Chen, Z., Zhang, L., 2014. Regional patterns of ^{15}N natural abundance in forest ecosystems along a large transect in eastern China. Sci. Rep. 4 (1), 4249. https://doi.org/10.1038/srep04249.
Shi, Y., Zhang, X., Wang, Z., Xu, Z., He, C., Sheng, L., Liu, H., Wang, Z., 2021. Shift in nitrogen transformation in peatland soil by nitrogen inputs. Sci. Total Environ. 764, 142924. https://doi.org/10.1016/j.scitotenv.2020.142924.
Skiba, U., Hergoualc'h, K., Drewer, J., Meijide, A., Knohl, A., 2020. Oil palm plantations are large sources of nitrous oxide, but where are the data to quantify the impact on global warming? Curr. Opin. Environ. Sustain. 47, 81–88. https://doi.org/10.1016/j.cosust.2020.08.019.
Sousa, J.R., Cabral, F., Coutinho, J., 2016. Assessment of N mineralization and N leaching in soil using a new in situ incubation method. Commun. Soil Sci. Plant Anal. 47 (19), 2157–2167. https://doi.org/10.1080/00103624.2016.1208751.
Stenstrom, M.K., Poduska, R.A., 1980. The effect of dissolved oxygen concentration on nitrification. Water Res. 14 (6), 643–649. https://doi.org/10.1016/0043-1354(80)90122-0.
Tang, A.C.I., Melling, L., Stoy, P.C., Musin, K.K., Aeries, E.B., Waili, J.W., Shimizu, M., Poulter, B., Hirata, R., 2020. A Bornean peat swamp forest is a net source of carbon dioxide to the atmosphere. Glob. Change Biol. 26 (12), 6931–6944. https://doi.org/10.1111/gcb.15332.
Tang, A.C.I., Stoy, P.C., Hirata, R., Musin, K.K., Aeries, E.B., Wenceslaus, J., Shimizu, M., Melling, L., 2019. The exchange of water and energy between a tropical peat forest and the atmosphere: seasonal trends and comparison against other tropical rainforests. Sci. Total Environ. 683, 166–174. https://doi.org/10.1016/j.scitotenv.2019.05.217.
Tarmizi, A.M., Mohd Tayeb, D., 2006. Nutrient demands of tenera oil palm planted on inland soil of Malaysia. Journal of Oil Palm Research 18, 204.
Tonks, A.J., Aplin, P., Beriro, D.J., Cooper, H., Evers, S., Vane, C.H., Sjögersten, S., 2017. Impacts of conversion of tropical peat swamp forest to oil palm plantation on peat organic chemistry, physical properties and carbon stocks. Geoderma 289, 36–45. https://doi.org/10.1016/j.geoderma.2016.11.018.
Verchot, L., Holmes, Z., Mulon, L., Groffman, P., Lovett, G., 2001. Gross vs net rates of N mineralization and nitrification as indicators of functional differences between forest types. Soil Biol. Biochem. 33 (14), 1889–1901. https://doi.org/10.1016/S0038-0717(01)00095-5.
Wang, C., Wang, N., Zhu, J., Liu, Y., Xu, X., Niu, S., Yu, G., Han, X., He, N., 2018. Soil gross N ammonification and nitrification from tropical to temperate forests in eastern China. Funct. Ecol. 32 (1), 83–94. https://doi.org/10.1111/1365-2435.13024.
Wangari, E.G., Mwanake, R.M., Houska, T., Kraus, D., Kikowatz, H.-M., Wolf, B., Gettel, G.M., Breuer, L., Ambus, P., Kiese, R., Butterbach-Bahl, K., 2024. Spatial-temporal patterns of foliar and bulk soil ^{15}N isotopic signatures across a heterogeneous landscape: Linkages tl soil N status, nitrate leaching, and N_2O fluxes. Soil Biol. Biochem. 199, 109609. https://doi.org/10.1016/j.soilbio.2024.109609.
Wangari, E.G., Mwanake, R.M., Kraus, D., Werner, C., Gettel, G.M., Kiese, R., Breuer, L., Butterbach-Bahl, K., Houska, T., 2022. Number of chamber measurement locations for accurate quantification of landscape-scale greenhouse gas fluxes: importance of land use, seasonality, and greenhouse gas type. J. Geophys. Res. Biogeosci. 127 (9). https://doi.org/10.1029/2022JG006901.
Wong, G.X., Hirata, R., Hirano, T., Kiew, F., Waili, J.W., Mander, Ü., Soosaar, K., Melling, L., 2025. Impact of land conversion on environmental conditions and methane emissions from a tropical peatland. Sci. Total Environ. 962, 178466. https://doi.org/10.1016/j.scitotenv.2025.178466.
Yin, T., Feng, M., Qiu, C., Peng, S., 2022. Biological nitrogen fixation and nitrogen accumulation in peatlands. Front. Earth Sci. 10. https://doi.org/10.3389/feart.2022.670867.
Zhang, Y., Liu, X., Liang, C., Wang, C., Wang, S., Zhang, J., Li, M., Shen, H., Tian, D., Bai, E., Zhu, J., Niu, S., Yu, G., Luo, Y., 2024. Global evidence for joint effects of multiple natural and anthropogenic drivers on soil nitrogen cycling. Glob. Change Biol. 30 (5), e17309. https://doi.org/10.1111/gcb.17309.